

Relationship between Structure, Entropy and Diffusivity in Water and Water-like Liquids

Manish Agarwal¹, Murari Singh[†], Ruchi Sharma¹ and Mohammad Parvez Alam¹
and Charusita Chakravarty^{1*}

November 4, 2018

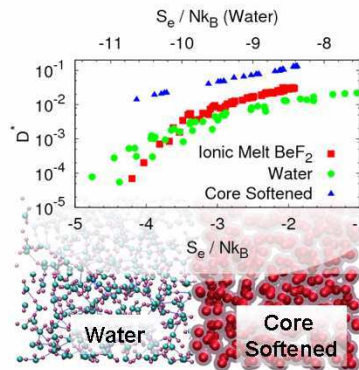
¹Department of Chemistry, Indian Institute of Technology-Delhi, New Delhi: 110016, India.

[†]School of Physical Sciences, Jawaharlal Nehru University, New Delhi: 110067, India

*Tel:(+)91-11-2659-1510 Fax:(+)91-11-2686-2122 E-mail:charus@chemistry.iitd.ernet.in

Abstract

Anomalous behaviour of the excess entropy (S_e) and the associated scaling relationship with diffusivity are compared in liquids with very different underlying interactions but similar water-like anomalies: water (SPC/E and TIP3P models), tetrahedral ionic melts (SiO_2 and BeF_2) and a fluid with core-softened, two-scale ramp (2SRP) interactions. We demonstrate the presence of an excess entropy anomaly in the two water models. Using length and energy scales appropriate for onset of anomalous behaviour, the density range of the excess entropy anomaly is shown to be much narrower in water than in ionic melts or the 2SRP fluid. While the reduced diffusivities (D^*) conform to the excess entropy scaling relation, $D^* = A \exp(\alpha S_e)$ for all the systems (Y. Rosenfeld, Phys. Rev. A **1977**, *15*, 2545), the exponential scaling parameter, α , shows a small isochore-dependence in the case of water. Replacing S_e by pair correlation-based approximants accentuates the isochore-dependence of the diffusivity scaling. Isochores with similar diffusivity scaling parameters are shown to have the temperature dependence of the corresponding entropic contribution. The relationship between diffusivity, excess entropy and pair correlation approximants to the excess entropy are very similar in all the tetrahedral liquids.



Keywords: Rosenfeld scaling, transport properties, excess entropy, water, water-like anomalies, silica, liquid-state anomalies, pair correlation entropy, tetrahedral liquids, core-softened fluids

1 Introduction

Water displays a number of thermodynamic and kinetic anomalies when compared to simple liquids [1–3]. The density anomaly, corresponding to a negative isobaric thermal expansion coefficient (α_P), is the best known of these unusual properties of water and is observed for state points lying within an approximately parabolic boundary defined by the locus of temperatures of maximum density (TMD) for which $\alpha_P = 0$. The density anomaly implies the presence of other thermodynamic anomalies, such as those associated with the isobaric heat capacity (C_p) and the isothermal compressibility (κ_T). The kinetic anomalies of water are associated with an increase in molecular mobility on isothermal compression, measured in terms of diffusivity, orientational relaxation times or viscosity. A number of network-forming inorganic melts with local tetrahedral order have been shown possess water-like anomalies, most notably, AB_2 ionic melts such as SiO_2 and BeF_2 and the liquid phase of elements, such as silicon and tellurium [4–15]. More recently, water-like anomalies have been demonstrated in mesoscopic liquids with isotropic, core-softened effective interactions or anisotropic patchy interactions [16–18]. Despite a very diverse set of underlying interactions, liquids with water-like anomalies are found to have essentially conformal liquid-state “phase diagrams” with a nested structure of anomalous regimes of density, diffusivity and structural order.

The similarity in the phase diagrams of water-like liquids reflects similar structure-entropy-diffusivity relationships that can be conveniently analysed in terms of the excess entropy, S_e , defined as the difference between the total thermodynamic entropy (S) and the corresponding ideal gas entropy (S_{id}) at the same temperature and density. A necessary condition for a fluid to show water-like thermodynamic and transport anomalies is the existence of an excess entropy anomaly, corresponding to a rise in excess entropy, S_e , on isothermal compression ($(\partial S_e / \partial \rho)_T > 0$) [9–11, 19–25]. Liquids with water-like anomalies display distinct forms of local order or length scales in the low- and high-density regimes; competition between the two types of local order results in a rise in excess entropy at intermediate densities. Most liquids, including anomalous ones, obey semi-quantitative excess entropy scaling relationships for transport properties of the form $X^* = A \exp(\alpha S_e)$ where X^* are reduced transport coefficients, and A and α are scaling parameters that are very similar for systems with conformal potentials [26–29]. Consequently, the existence of an excess entropy anomaly is reflected in mobility anomalies. In

order to make a more precise connection between thermodynamic and mobility anomalies, it is necessary to understand the assumptions underlying the scaling rule. Rosenfeld-scaling assumes that diffusion in liquids takes place through a combination of binary collisions and cage relaxation. The binary collision contribution is approximately factored out by using macroscopic reduction parameters based on elementary kinetic theory. For example, reduced diffusivities are defined as $D^* = D(\rho^{1/3}/(mk_B T)^{1/2})$ [27]. The frequency of cage relaxations is assumed to be proportional to the number of accessible configurations, $\exp(\alpha S_e)$, since configuration space connectivity is high in the stable liquid phase. In order for the scaling relationship to be state-point independent, it is necessary that the exponential parameter α controlling the number of accessible configurations is determined by the interaction potential and is otherwise state-point independent.

This paper develops a basis for quantitative comparison of structure-entropy-diffusivity relationships in liquids with very different underlying interactions but similar water-like anomalies. We focus on three different categories of liquids: (i) molecular fluids (H_2O), (ii) tetrahedral ionic melts (BeF_2 and SiO_2) and a core-softened fluid with isotropic, pair-additive interactions. Comparison of these different systems should provide very useful physical insights into the relationship between structure, entropy and transport properties of liquids, including complex fluids, and has not been previously attempted. It is evident that parametric variations of a single functional form for the interaction potential are insufficient to serve as a basis for comparison of anomalous behaviour for the three different categories of liquids studied here. Instead, we focus on directly comparing the two crucial features of the excess entropy relevant for water-like liquids: firstly, the presence of an excess entropy anomaly and secondly, exponential scaling of transport properties with excess entropy. Since the state point, (ρ_m, T_m) , corresponding to the maximum temperature along the TMD locus is a unique point common to all liquids with a water-like density anomaly, we use this information to define a natural energy and length scale for onset of anomalous behaviour in each system.

The specific interaction models used for the different categories of liquids require some introductory comments. Anomalous behaviour and scaling of transport properties with the thermodynamic excess entropy has so far not been studied in the case of water. Since the different water models are known to display anomalous properties at very different temperatures,

we use two different effective pair potentials for water, TIP3P and SPC/E. The SPC/E model is known to qualitatively reproduce all anomalous properties of water but typically at temperatures that are 30K to 40K lower than the experimental value of 279K [2–4, 19, 30]. The TIP3P model is widely used in biomolecular simulations, but the onset temperature for anomalous behaviour is 170-180K [19, 31, 32]. The transferable rigid-ion model (TRIM) potential was used for BeF₂ [33] and the van Beest-Kramer-van Santen (BKS) potential was used for SiO₂ [34]. As an example of a core-softened fluid with waterlike anomalies, we consider the two-scale ramp potential (2SRP) [16, 17]. Thus we study five different simulation models for the three categories of liquids. Table 1 summarises some of the relevant information about these simulation systems at (ρ_m, T_m) . Section 2 provides the necessary simulation details. Results are presented in Section 3 and conclusions are discussed in section 4.

2 Simulation Details

Potential energy models for all systems studied here are given in Table 1. Molecular dynamics simulations of ionic melts (BeF₂ and SiO₂) and water models (TIP3P and SPC/E) were performed in the NVT ensemble using the Verlet algorithm as implemented in the DL_POLY package [35]. Temperature range of 1500-3000K is studied for BeF₂ and 4000-6000K for SiO₂. Details of simulations of the two ionic melts are given in ref. [36]. Simulations of TIP3P and SPC/E water used 256 molecules in a cubic simulation box with 1 fs timestep and production run lengths of 4 to 8 ns. Rigid-body constraints were maintained using the SHAKE algorithm. The Berendsen thermostat time constant, τ_B , is 1ps for SPC/E for all state points except those along the 210K isotherm ($\tau_B=200$ ps) while $\tau_B=20$ ps for all TIP3P state points. State points for SPC/E water covered a temperature range from 210K to 300K and density range from 0.9 g cm⁻³ to 1.4 g cm⁻³; the temperature range for TIP3P water was kept as 170K to 300K.

Simulations of the two-scale ramp potential (2SRP) fluid were performed using Metropolis Monte Carlo simulations using 256 particles in a cubic simulation box. The 2SRP fluid has length scales associated with the hard-core (σ_0) and soft-core (σ_1) diameters; we use σ_1 as the unit of length. The energy U_1 of the linear ramp interaction extrapolated to zero separation is taken as the unit of energy. State points cover a temperature range of 0.025 to 0.2 and density range from 0.8 to 2.6 in reduced units [9]). Diffusivities for five isotherms from $T = 0.027$ to $T = 0.063$ were taken from ref. [37].

Widom insertion method was used to calculate chemical potential and excess entropy for the 2-scale ramp fluid at low densities and high temperatures [38]. Thermodynamic integration was then used to obtain excess entropies at other statepoints. For ionic melts, S_{id} is computed for a non-interacting multi-component mixture of atoms with the same masses and mole fractions as the ionic melt. Excess entropy for BeF_2 and SiO_2 melts were calculated using the same procedure as in ref [19], but over a more extensive density range. The excess entropy of the water models was computed relative to an ideal gas of rigid triatomic molecules at 1000K, 0.01g/cc. Thermodynamic integration was used to compute S_e at other state points [4]. Our entropies at 298K and 1 g cm⁻³ match those of [39] for SPC/E and TIP3P, within statistical error. The use of atom-atom RDFs in equation(1) would suggest that an ideal gas reference state analogous to that used for ionic melts would be more appropriate; this is in fact not necessary, since the difference between the two reference states will be constant at a given temperature and density. We note that while the system sizes chosen were chosen to be small enough that a large number of state points could be efficiently covered, they are sufficiently big that finite-size effects would be expected to make only small quantitative differences to the computed values of thermodynamic and transport properties.

3 Results

3.1 Excess Entropy Anomaly

The strength of the excess entropy anomaly determines the presence of diffusional, density and related anomalies and reflects the variation in structural order in a fluid as a function of density. Figure 1 compares the density dependence of the excess entropy along the $T = T_m$ isotherm, scaling densities with respect to the ρ_m value of each system. While the overall behaviour of $S_e(\rho/\rho_m)$ is very similar, it is immediately apparent that, in units of ρ_m , the water models have a relatively narrow density regime of anomalous behaviour and a steeper slope in the high density regime. The two-scale ramp (2SRP) system in contrast, has a much wider anomalous regime bounded by a well-defined minimum as well as maximum in $S_e(\rho)$ along the T_m isotherm. The two ionic melts resemble the ramp fluid in the density range of anomalous behaviour and the location of the maximum in $S_e(\rho/\rho_m)$. The minimum in the $S_e(\rho/\rho_m)$ curves could not, however, be located within the density range consistent with the

thermodynamic stability criterion that the isothermal compressibility should be positive. In units of Nk_B , the rise in the $S_e(\rho)$ curves from the minimum to the maximum is a fraction of a k_B for all the systems. This small anomaly is, however, sufficient to create an inflexion point in the total $S(\rho) = S_{id} + S_e$ curves that marks the onset of the density anomaly. The qualitative behaviour of the excess entropy anomaly is consistent with the grouping of the fluids into three similar classes: rigid water models, ionic melts and core-softened fluids. Unless otherwise stated, results for only one member of each class will be discussed in the rest of this paper.

3.2 Excess Entropy Scaling of Diffusivities

A comparison of the excess entropy scaling of the diffusivities for the different systems studied in this work, shown in Figure 2, illustrates that such a scaling approach is a reasonable predictor of diffusivities though there are small system-dependent differences. The 2SRP fluid shows excellent scaling for the state points studied, but the range of variation of the diffusivities is small in comparison to both ionic melts and water, given temperature variations by factors of two to three. Both SiO_2 and BeF_2 show very good scaling in the liquid regime, but there is a change in slope α for the lowest temperature isotherms, possibly due to onset of cooperative dynamics [21, 22, 36, 40, 41]. The water models all show a distinct isochore dependence of the $\ln D^*$ versus S_e plots, which is less pronounced in ionic melts and is essentially zero in the 2SRP fluid. In the case of water, deviations from linearity are specially noticeable at low temperatures for the 0.90 and 1.40 g cm^{-3} isochores for which the mode-coupling temperature is relatively high [42]. All liquids with water-like anomalies are associated with a competition between two different length scales or local order metrics as a function of density. Therefore deviations from corresponding states behaviour would be expected. It appears, however, that these deviations are small and most noticeable in the case of water which has a rigid, non-spherical structure. Possible reasons for this are discussed below.

3.3 Pair Correlation Estimators of the Excess Entropy

The effect of the underlying structural correlations in a fluid on the entropy-transport relationships can be understood by expressing S_e as a multiparticle correlation expansion, $S_e = S_2 + S_3 + \dots$, where S_n is the entropy contribution due to n -particle spatial correla-

tions [43–45]. The entropy contribution due to pair correlations between atoms of type α and β is given by:

$$S_{\alpha\beta} = \int_0^\infty \{g_{\alpha\beta}(r) \ln g_{\alpha\beta}(r) - [g_{\alpha\beta}(r) - 1]\} r^2 dr \quad (1)$$

where $g_{\alpha\beta}(r)$ is the atom-atom pair distribution function (PDF). The overall pair correlation entropy, S_2 , is: $S_2/Nk_B = -2\pi\rho \sum_{\alpha,\beta} x_\alpha x_\beta S_{\alpha\beta}$ where N is the number of particles and x_α is the mole fraction of component α in the mixture. S_2 can be estimated from experimental scattering data as well as simulations and is the dominant contribution to the excess entropy in the case of simple [44] and core-softened fluids (e.g. results for 2SRP fluid in this paper), ionic melts and water [19]. In the case of the AB_2 melts and water, we also compute the tetrahedral correlation entropy, S_{AA} , due to the pair correlations between the tetrahedral(A) atoms, corresponding to Be, Si and O in BeF_2 , SiO_2 and H_2O respectively. The S_{OO} entropic contribution is reproduced by many coarse-grained model potentials of water that replace each water molecule by a structureless particle with isotropic effective interactions that reproduce the behaviour of $g_{OO}(r)$ [46,47].

3.3.1 Diffusivity Scaling

The effect of using a structure-based approximant to the excess entropy, such as S_2 , on the Rosenfeld-scaling relation can be seen by substituting $S_e = S_2 + \Delta S$ to obtain

$$D^* \approx A \exp(\alpha S_e) = A \exp[\alpha S_2(1 + \Delta S/S_2)] = A \exp(\alpha' S_2) \quad (2)$$

where the new exponential scaling parameter, $\alpha' = 1 + \Delta S/S_2$, has a state-point dependence that is determined by the density and temperature-dependent behaviour of $\Delta S/S_2$. Thus by using different approximants to the excess entropy and observing the effect on the scaling behaviour of the transport properties, one can determine importance of different structural correlations in controlling mobility. Figure 3 shows the correlation between the dimensionless diffusivity (D^*) and S_2 as well as $x_{OO}^2 S_{OO}$ for SPC/E water, which should be compared with Figure 2(a). It is immediately obvious that the temperature dependence along an isochore is linear or quasi-linear, but there is a distinct isochore dependence of the slope α of the $\ln D^*$ versus S_μ plots. The isochore-dependence is most pronounced for $S_\mu = S_{OO}$ and least pronounced for

$S_\mu = S_e$. While the $\ln D^*$ versus S_2 or S_{AA} behaviour has been studied before [12, 23, 25, 36], no systematic comparison with S_e and S_2 scaling has been made so far. The ionic melts show a parallel behaviour to the water models, in terms of diffusivity scaling with respect to S_e , S_2 and S_{AA} while the 2SRP fluid also shows a small isochore dependence when D^* is scaled with respect to S_2 . In the case of BeF_2 , the diffusivity and viscosity scaling with respect to S_e and S_2 is given in refs. [12, 36] and with respect to S_{BeBe} in Supporting Information Figures 1. Scaling with respect to both S_e and S_2 for 2SRP fluid is shown in Supporting Information Figure 2. This is in contrast to simple liquids with pair additive potentials for where excess entropy scaling relationships based on S_e and S_2 have a similar degree of universality [28].

3.3.2 Temperature Dependence

The isochore-dependence of diffusivity scaling with different entropic contributions, and the contrast with simple liquids, suggests that the isochoric temperature dependence of different entropic measures determines the quality of entropy-diffusivity scaling. Based on measure-free density functional theory for repulsive potentials, Rosenfeld predicted a $T^{-2/5}$ scaling for the excess entropy [48]. In the case of simple liquids, these predictions are satisfied by both S_e and S_2 and Rosenfeld-scaling holds very well [48, 49]. S_e is known to show $T^{-2/5}$ scaling in ionic melts and water over temperature regime of interest in this study [4, 6]. Figure 4 shows S_e , S_2 and S_{OO} as a function of $T^{-2/5}$ for different isochores in SPC/E water. Unlike in simple liquids, S_2 and S_{OO} show significant deviations from $T^{-2/5}$ scaling in the anomalous regime. The results for BeF_2 are very similar to those of SPC/E water (see Supporting Information Figure 3 and ref. [10, 19]). In the case of the 2SRP fluid, both S_e and S_2 show deviations from $T^{-2/5}$ behaviour at low temperatures (see Supporting Information Figure 4).

A comparison of the isochore-dependence of the Rosenfeld-scaling parameter with respect to an entropic contribution, S_μ , and the temperature dependence of S_μ shows that isochores with very different temperature dependences also have very different diffusivity scaling parameters. For example, Figure 3(b) shows when $\ln D^*$ is plotted as a function of S_{OO} , then the slope increases with increasing density and the three densest isochores, at $\rho = 1.2, 1.3$ and 1.4 g cm^{-3} show very different and progressively increasing values of α . Figure 4(c) shows that S_{OO} along these three isochores has a distinctly different and very weak temperature dependence. The two

AB₂ ionic melts show a very similar pattern of behaviour (see Supporting Information Figures 1 and 3), reflecting the similar structure of the tetrahedral fluids. The 2SRP fluid shows a weak isochore dependence of α when S_e is replaced by S_2 , which may be related to a wider spread of S_2 values compared with S_e . It is interesting to note that $S_2(T)$ and $S_{AA}(T)$ curves show a much stronger density dependence than $S_e(T)$. In the case of the tetrahedral liquids, it is notable that at high densities, S_{AA} remains almost constant with temperature while diffusivity rises quite sharply. Since the overall excess entropy scaling for high and low density isotherms is not qualitatively different, this must imply that significant reorganisation of the network associated with the other pair correlation contributions contributes to controlling diffusivity; for example, in water this could be strong librational-translational coupling reflected in the S_{OH} and S_{HH} contributions.

4 Discussion and Conclusions

The excess entropy anomaly is compared in five liquids with water-like anomalies, with three completely different types of interactions: ionic melts (BeF₂ and SiO₂), hydrogen-bonded molecular liquid (SPC/E and TIP3P water), core-softened fluid (two-scale ramp). Using the state point, (ρ_m, T_m) , corresponding to the maximum temperature along the TMD locus to define energy and length scales, we show that excess entropy anomaly in the ionic melts and the core-softened fluid is very similar in range and strength, while the two water models have a conspicuously smaller density range and a much sharper decrease in S_e with density on strong compression.

We show that scaling of diffusivities with the thermodynamic excess entropy is good in all cases, noting that water is the first molecular fluid, other than the Lennard-Jones chain fluid [50], for which Rosenfeld-scaling with the thermodynamic excess entropy, rather than pair-correlation based estimators, has been tested. In comparison to ionic melts and the 2SRP fluid, a small isochoric dependence of the Rosenfeld-scaling parameters is seen in the case of water. This suggests the presence of additional length scales due to the rigid, non-spherical molecular shape, but these are not critical enough to destroy the overall correlation. The results for water suggest that Rosenfeld-scaling will be useful for many other molecular fluids as a predictor of dynamical properties.

We examine the diffusivity scaling with two different entropy estimators based on pair

correlation distribution functions (PDFs). The first one which we refer to as the pair correlation entropy, S_2 , includes information from all atom-atom PDFs. The second one, referred to as the tetrahedral correlation entropy (S_{AA}), considers only the contribution from the pair correlations between the tetrahedral atom-atom PDFs and is applicable to only water and ionic melts. We show that the isochore dependence of the diffusivity scaling parameters is most pronounced for S_{AA} , much less pronounced for S_2 and virtually negligible for S_e . Thus the state-dependence of Rosenfeld scaling parameters increases as the structural approximants to the entropy become poorer. We demonstrate that isochores with similar temperature-dependence of the entropy estimators show very similar Rosenfeld-scaling parameters.

The clear correspondence between the isochoric Rosenfeld-scaling parameters and the temperature dependence of the entropy along isochores has an interesting implication. The isochoric temperature dependence of the excess entropy of many atomic systems obeys a $T^{-2/5}$ scaling, possibly because of the critical role of strong, short-range repulsions [48]. S_2 shows a similar $T^{-2/5}$ dependence in simple liquids but not in anomalous fluids, as shown in this study and elsewhere [11,19,49]. This suggests that diffusivities for many atomic fluids will obey Rosenfeld-scaling best when the thermodynamic excess entropy is used. The 2SRP fluid presents an interesting case in that Rosenfeld-scaling is applicable though there are deviations from $T^{-2/5}$ scaling. It would be interesting to examine these ideas in the context of recent work on strongly correlating fluids [51,52].

Our results on structure-entropy-diffusivity relationships are experimentally testable. Atom-atom PDFs, diffusivities and calorimetric entropy are experimentally accessible as a function of temperature and density (or pressure). A comparison of diffusivity scaling with the thermodynamic entropy as well as the O-O pair correlation entropy between water and methanol should itself be very interesting, because they are both molecular, hydrogen-bonded liquids. Methanol, unlike water, does not show pronounced liquid state anomalies and we expect that this will show up in the diffusivity scaling with respect to the oxygen-oxygen pair correlation entropy but not with respect to the thermodynamic excess entropy. Since the atom-atom RDFs can be measured for essentially all molecular and polymeric fluids, our results suggest that excess entropy scaling should have substantial predictive value when combined with structural data, provided the complete set of atom-atom RDFs is used for estimating the entropy. However, coarse-graining

procedures which rely on mapping a subset of atom-atom PDFs will not necessarily preserve the thermodynamic state-point dependence of transport properties, specially in anomalous fluids, as has been noted in recent studies of coarse-grained potentials for water [46, 47].

Our results suggest that Rosenfeld-scaling is valid for a wide range of simple and anomalous liquids. The deviations are small if the complete thermodynamic excess entropy is used, possibly because of the dominance of strong, short-range repulsions. A microscopic understanding of Rosenfeld-scaling is, however, necessary in order to understand the occurrence and magnitude of deviations in different systems. One possible route to developing such a microscopic approach is to use energy landscape approaches that have proved very useful in the context of supercooled liquids [53, 54]. Efforts to apply energy landscape analysis to understand Rosenfeld-scaling in simple and anomalous liquids have been relatively few [46, 55, 56].

Water-like liquids are systems where an additional length scale comes into play as a function of density and therefore deviations from Rosenfeld-scaling may be expected. As discussed in this paper, deviations are, in fact, small in this case. An analogous set of systems could be those where an additional length scale emerges as a function of temperature, as in inverse melting systems [57]. Some of the recent work on Rosenfeld-scaling in systems with finite repulsions, such as the Hertzian sphere and the Gaussian-core [58–61], can be understood in terms of deviations from Rosenfeld-scaling behaviour due to change in the character of binary collisions as well as the possibility of additional length scales as a function of density.

To summarize, the anomalous behaviour of the excess entropy (S_e) and the associated scaling relationship with diffusivity is compared in five liquids with water-like thermodynamic and transport anomalies: SPC/E and TIP3P water models, SiO₂ and BeF₂ ionic melts and the two-scale ramp (2SRP) fluid. By defining suitable length and energy scales for onset of anomalous behaviour, the density range of the excess entropy anomaly in water is shown to be much narrower in water than in ionic melts or the 2SRP fluid. While the Rosenfeld prediction of an exponential dependence of reduced diffusivity (D^*) on the excess entropy (S_e), $D^* = A \exp(\alpha S_e)$ is found to be almost quantitatively valid for all the systems, the exponential scaling parameter, α , is found to show a small isochore-dependence in the case of water, presumably due to the rigid molecular structure. Unlike in the case of simple liquids, this isochore-dependence of the excess entropy scaling of the diffusivities is accentuated by replacing S_e by the pair

correlation entropy, S_2 , for all the systems. In the case of the AB_2 ionic melts and water, the effect is more pronounced if the diffusivity is scaled with respect to the pair correlation entropy associated with the tetrahedral atoms. More interestingly, variations in the isochoric temperature dependence of the entropic contribution (S_e , S_2 and S_{AA}) are found to be correlated with variations in the isochore diffusivity scaling parameters, suggesting that the organisation of the energy landscape changes significantly with density. The tetrahedral liquids (ionic melts and water) show very similar structure-entropy-diffusivity relations. Our results suggest that by systematically considering systems which represent different types and degrees of deviation from assumptions underlying Rosenfeld-scaling, interesting physical insights into the relationship between structure, thermodynamics and transport in liquids can be obtained.

Acknowledgements This work was financially supported by the Department of Science and Technology, New Delhi. MA would like to thank Indian Institute of Technology-Delhi for award of a Senior Research Fellowship. MS would like to thank University Grants Commission, New Delhi for award of a Junior Research Fellowship. The authors thank Divya Nayar for assistance with some of the computations.

Supporting Information Available: Additional figures, referenced in the text to support our conclusions, are available free of charge via the Internet at <http://pubs.acs.org>.

References and Notes

- (1) Mishima, O.; Stanley, H. E. The relationship between liquid, supercooled and glassy water. *Nature* **1998**, *396*, 329–335.
- (2) Debenedetti, P. G. Supercooled and glassy water. *J. Phys-Cond. Matt.* **2003**, *15*, R1669–R1726.
- (3) Errington, J. R.; Debenedetti, P. G. Relationship between structural order and the anomalies of liquid water. *Nature* **2001**, *409*, 318–321.
- (4) Scala, A.; Starr, F. W.; Nave, E. L.; Sciortino, F.; Stanley, H. E. Configurational entropy and diffusivity of supercooled water. *Nature* **2000**, *406*, 166–169.
- (5) Shell, M. S.; Debenedetti, P. G.; Panagiotopoulos, A. Z. Molecular structural order and anomalies in liquid silica. *Phys. Rev. E.* **2002**, *66*, 011202.

- (6) Poole, P. H.; Hemmati, M.; Angell, C. A. Comparison of thermodynamic properties of simulated liquid silica and water. *Phys. Rev. Lett.* **1997**, *79*, 2281–2284.
- (7) Hemmati, M.; Moynihan, C. T.; Angell, C. A. Interpretation of the molten BeF₂ viscosity anomaly in terms of a high temperature density maximum, and other waterlike features. *J. Chem. Phys.* **2001**, *115*, 6663–6671.
- (8) Tanaka, H. Simple view of waterlike anomalies of atomic liquids with directional bonding. *Phys. Rev. B* **2002**, *66*, 064202.
- (9) Sharma, R.; Chakraborty, S. N.; Chakravarty, C. Entropy, diffusivity, and structural order in liquids with waterlike anomalies. *J. Chem. Phys.* **2006**, *125*, 204501.
- (10) Agarwal, M.; Sharma, R.; Chakravarty, C. Ionic melts with waterlike anomalies: Thermodynamic properties of liquid BeF₂. *J. Chem. Phys.* **2007**, *127*, 164502.
- (11) Agarwal, M.; Chakravarty, C. Waterlike structural and excess entropy anomalies in liquid beryllium fluoride. *J. Phys. Chem. B* **2007**, *111*, 13294–13300.
- (12) Agarwal, M.; Chakravarty, C. Relationship between structure, entropy, and mobility in network-forming ionic melts. *Phys. Rev. E* **2009**, *79*, 030202.
- (13) Molinero, V.; Moore, E. B. Water modeled as an intermediate element between carbon and silicon. *J. Phys. Chem. B* **2009**, *113*, 4008–4016.
- (14) Sastry, S.; Angell, C. A. Liquid-liquid phase transition in supercooled silicon. *Nature Mat.* **2003**, *2*, 739–743.
- (15) Kanno, H.; Yokoyama, H.; Yoshimura, Y. A new interpretation of anomalous properties of water based on Stillinger’s postulate. *J. Phys. Chem. B* **2001**, *105*, 2019–2026.
- (16) Jagla, E. A. Low-temperature behavior of core-softened models: Water and silica behavior. *Phys. Rev. E* **2001**, *63*, 061509.
- (17) Yan, Z.; Buldyrev, S. V.; Giovambattista, N.; Stanley, H. E. Structural order for one-scale and two-scale potentials. *Phys. Rev. Lett.* **2005**, *95*, 130604.

- (18) Sciortino, F. Gel-forming patchy colloids and network glass formers: thermodynamic and dynamic analogies. *Euro. Phys. J. B* **2008**, *64*, 505–509.
- (19) Sharma, R.; Agarwal, M.; Chakravarty, C. Estimating entropy of liquids from atom-atom radial distribution functions: Silica, beryllium fluoride and water. *Mol. Phys.* **2008**, *106*, 1925–1938.
- (20) de Oliveira, A. B.; Franzese, G.; Netz, P. A.; Barbosa, M. C. Waterlike hierarchy of anomalies in a continuous spherical shouldered potential. *J. Chem. Phys.* **2008**, *128*, 064901.
- (21) Mittal, J.; Errington, J. R.; Truskett, T. M. Relationship between thermodynamics and dynamics of supercooled liquids. *J. Chem. Phys.* **2006**, *125*, 076102.
- (22) Mittal, J.; Errington, J. R.; Truskett, T. M. Erratum: Relationship between thermodynamics and dynamics of supercooled liquids [JCP 125, 076102 (2006)]. *J. Chem. Phys.* (to be published).
- (23) Mittal, J.; Errington, J. R.; Truskett, T. M. Quantitative link between single-particle dynamics and static structure of supercooled liquids. *J. Phys. Chem. B* **2006**, *110*, 18147–18150.
- (24) Errington, J. R.; Truskett, T. M.; Mittal, J. Excess-entropy-based anomalies for a waterlike fluid. *J. Chem. Phys.* **2006**, *125*, 244502.
- (25) Yan, Z.; Buldyrev, S. V.; Stanley, H. E. Relation of water anomalies to the excess entropy. *Phys. Rev. E* **2008**, *78*, 051201.
- (26) Rosenfeld, Y. Relation between transport coefficients and the internal energy of simple systems. *Phys. Rev. A* **1977**, *15*, 2545–2549.
- (27) Rosenfeld, Y. A quasi-universal scaling law for atomic transport in simple fluids. *J. Phys-Cond. Matt.* **1999**, *11*, 5415.
- (28) Dzугutov, M. A universal scaling law for atomic diffusion in condensed matter. *Nature (London)* **1996**, *381*, 137–139.
- (29) Hoyt, J. J.; Asta, M.; Sadigh, B. Test of the universal scaling law for the diffusion coefficient in liquid metals. *Phys. Rev. Lett.* **2000**, *85*, 594–597.

- (30) Berendsen, H. J. C.; Grigera, J. R.; Straatsma, T. P. The missing term in effective pair potentials. *J. Phys. Chem* **1987**, *91*, 6269–6271.
- (31) Jorgensen, W. L.; Chandrasekhar, J.; Madura, J. D.; Impey, R. W.; Klein, M. L. Comparison of simple potential functions for simulating liquid water. *J. Chem. Phys.* **1983**, *79*, 926–935.
- (32) Vega, C.; Abascal, J. L. F. Relation between the melting temperature and the temperature of maximum density for the most common models of water *J. Chem. Phys.* **2005**, *123*, 144504.
- (33) Woodcock, L. V.; Angell, C. A.; Cheeseman, P. Molecular dynamics studies of vitreous state: Simple ionic systems and silica. *J. Chem. Phys.* **1976**, *65*, 1565–1577.
- (34) van Beest, B. W. H.; Kramer, G. J.; van Santen, R. A. Force fields for silicas and aluminophosphates based on ab initio calculations. *Phys. Rev. Lett.* **1990**, *64*, 1955–1958.
- (35) Smith, W.; Yong, C. W.; Rodger, P. M. DL-POLY: Application to molecular simulation. *Mol. Simulat.* **2002**, *28*, 385–471.
- (36) Agarwal, M.; Ganguly, A.; Chakravarty, C. Transport properties of tetrahedral, network-forming ionic melts. *J. Phys. Chem. B* **2009**, *15284*, 113.
- (37) Kumar, P.; Buldyrev, S. V.; Sciortino, F.; Zaccarelli, E.; Stanley, H. E. Static and dynamic anomalies in a repulsive spherical ramp liquid: Theory and simulation. *Phys. Rev. E.* **2005**, *72*, 021501.
- (38) Frenkel, D.; Smit, B. *Understanding Molecular Simulation: From Algorithms to Applications.*; Academic Press: London, 2002.
- (39) Henchman, R. H. Free energy of liquid water from a computer simulation via cell theory. *J. Chem. Phys.* **2007**, *126*, 064504.
- (40) Dzugutov, M. Dynamical diagnostics of ergodicity breaking in supercooled liquids. *J. Phys.-Cond. Matt.* **1999**, *11*, A253.
- (41) Kaur, C.; Harbola, U.; Das, S. P. Nature of the entropy versus self-diffusivity plot for simple liquids. *J. Chem. Phys.* **2005**, *123*, 034501.

- (42) Starr, F. W.; Sciortino, F.; Stanley, H. E. Dynamics of simulated water under pressure. *Phys. Rev. E* **1999**, *60*, 6757–6768.
- (43) Green, H. S. *The Molecular Theory of Fluids.*; North-Holland, Amsterdam, 1952.
- (44) Baranyai, A.; Evans, D. J. Direct entropy calculation from computer simulation of liquids. *Phys. Rev. A* **1989**, *40*, 3817–3822.
- (45) Laird, B. B.; Haymet, A. D. J. Calculation of entropy from multiparticle correlation functions. *Phys. Rev. A* **1992**, *45*, 5680–5689.
- (46) Johnson, M. E.; Head-Gordon, T. Assessing thermodynamic-dynamic relationships for waterlike liquids. *J. Chem. Phys.* **2009**, *130*, 214510.
- (47) Chaimovich, A.; Shell, M. S. Anomalous waterlike behavior in spherically-symmetric water models optimized with the relative entropy *Phys. Chem. Chem. Phys.* **2009**, *11*, 1901–1915.
- (48) Roseneld, Y.; Tarazona, P. Density functional theory and the asymptotic high density expansion of the free energy of classical solids and fluids *Mol. Phys.* **1998**, *95*, 141–150.
- (49) Chakraborty, S. N.; Chakravarty, C. Entropy, local order, and the freezing transition in morse liquids. *Phys. Rev. E* **2007**, *76*, 011201.
- (50) Goel, T.; Patra, C. N.; Mukherjee, T.; Chakravarty, C. Excess entropy scaling of transport properties of Lennard-Jones chains. *J. Chem. Phys.* **2008**, *129*, 164904.
- (51) Gnan, N.; Schrder, T. B.; Pedersen, U. R.; Bailey, N. P.; Dyre, J. C.; Pressure-energy correlations in liquids. IV. Isomorphs in liquid phase diagrams. *J. Chem. Phys.* **2009**, *131*, 234504
- (52) Pedersen, U. R.; Bailey, N. P.; Schrder, T. B.; Dyre, J. C.; Strong Pressure-Energy Correlations in van der Waals Liquids. *Phys. Rev. Lett.* **2008**, *100*, 015701
- (53) Debendetti, P. G.; Stillinger, F. H. Supercooled liquids and the glass transition *Nature* **2001**, *410*, 259–267.
- (54) Karmakar, S.; Dasgupta, C.; Sastry, S. Growing length and time scales in glass-forming liquids. *Proc. Natl. Acad. Sci.* **2009**, *106*, 3675–3679.

- (55) Chakraborty, S. N.; Chakravarty, C.; Diffusivity, Excess Entropy and the Potential Energy Landscape of Monoatomic Liquids. *J. Chem. Phys.*, **2006**, *124*, 014507.
- (56) de Oliveira, A. B.; Salcedo, E.; Chakravarty, C.; Barbosa, M. C.; Entropy, diffusivity and the energy landscape of a water-like fluid. [arXiv:1002.3781v1](https://arxiv.org/abs/1002.3781v1) [`cond-mat.soft`]
- (57) Feeney, M. R.; Debenedetti, P. G.; Stillinger, F. H. A statistical mechanical model for inverse melting. *J. Chem. Phys.* **2003**, *119*, 4582–4591.
- (58) Krekelberg, W. P.; Kumar, T.; Mittal, J.; Errington, J. R.; Truskett, T. M. Anomalous structure and dynamics of the gaussian-core fluid. *Phys. Rev. E* **2009**, *79*, 031203.
- (59) Pamies, J. C.; Cacciuto, A.; Frenkel, D. Phase diagram of Hertzian spheres. *J. Chem. Phys.* **2009**, *131*, 044514.
- (60) Fomin, Y. D.; Gribova, N. V.; Ryzhov, V. N.; Breakdown of The Excess Entropy Scaling for the Systems with Thermodynamic Anomalies. [arXiv:1001.0111v1](https://arxiv.org/abs/1001.0111v1) [`cond-mat.soft`]
- (61) Krekelberg, W. P.; Pond, M. J.; Goel, G.; Shen, V. K.; Errington, J. R.; Truskett, T. M.; Generalized Rosenfeld scalings for tracer diffusivities in not-so-simple fluids: Mixtures and soft particles. *Phys. Rev. E*, **2009**, *80*, 061205.

Figures

1. Plot of excess entropy S_e with scaled number density, ρ/ρ_m for (a) ionic melts and 2SRP fluid and (b) water models. The lines mark the respective minima and maxima in the 2SRP fluid in part (a) and the SPC/E model in part (b).
2. Correlation plots of Rosenfeld-scaled diffusivities with excess entropy, S_e of (a) two-scale ramp potential (2SRP) fluid, (b) AB_2 Ionic Melts (BeF_2 and SiO_2) and (c) SPC/E and (d) TIP3P. The lowest isotherms for BeF_2 and SiO_2 are shown with filled symbols. Data points lying along the highest and lowest isochore for (c) and (d) are joined with smooth lines. The scaling parameter α for each plot is shown. In part (b), the datapoints at 1500K(BeF_2) and 4000K(SiO_2) are shown as filled symbols, and are excluded from the fit. In part (c) and (d), data points having $S_e < -9.5$ are excluded from the fit.
3. Correlation plots of Rosenfeld scaled diffusivities, D^* , in SPC/E water with: (a) S_2 (b) S_{OO} for selected isochores. Straight lines connect data from the highest and lowest density isochores.
4. Different entropic contributions in SPC/E as a function of $T^{-2/5}$: (a) thermodynamic excess entropy, S_e , (b) pair correlation entropy, S_2 and (c) entropic contribution due to oxygen-oxygen pair correlations, $x_o^2 S_{OO}$ with $T^{-2/5}$.

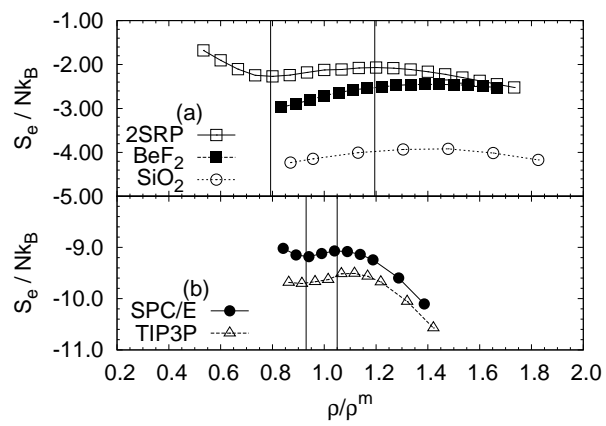


Figure 1.

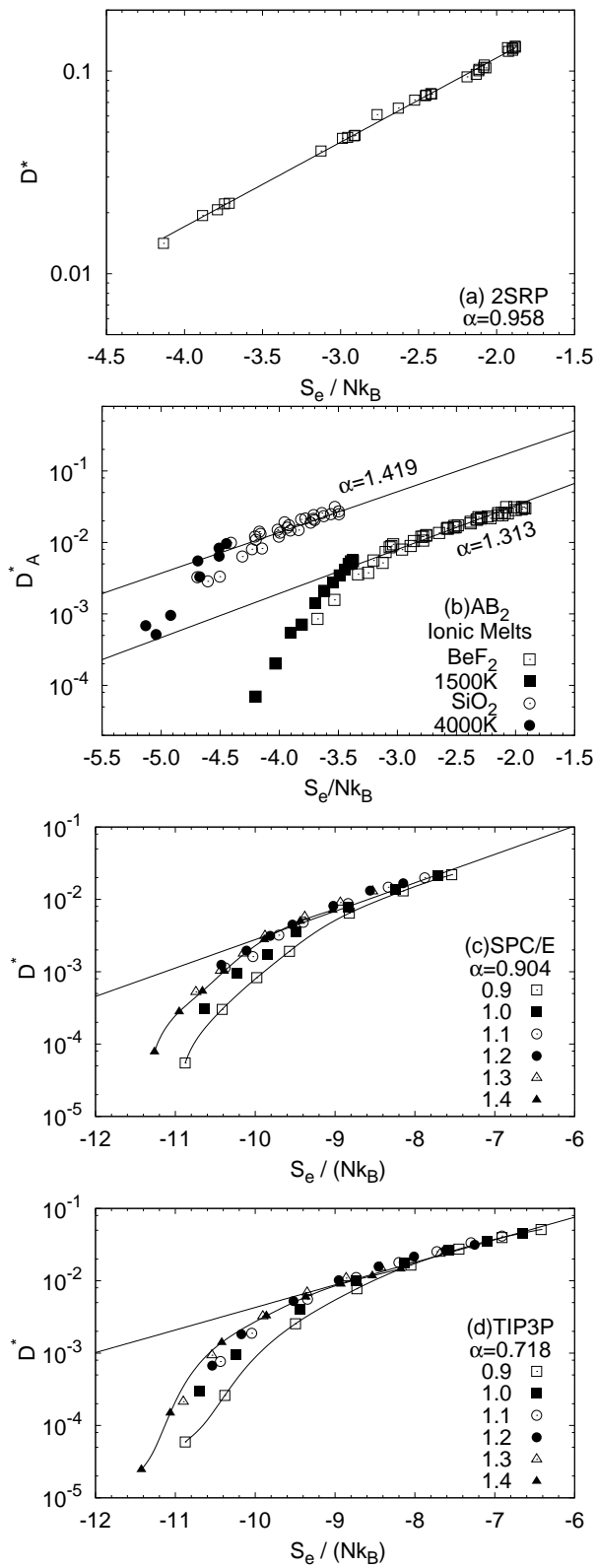


Figure 2.

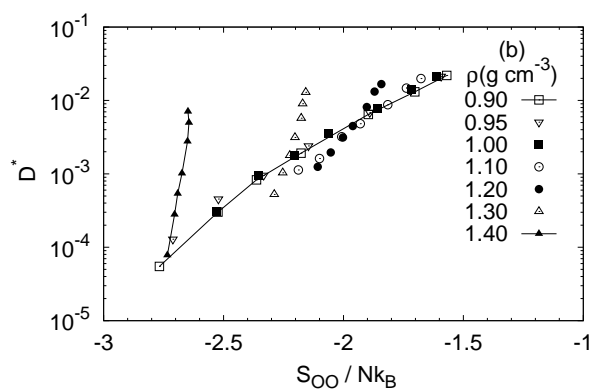
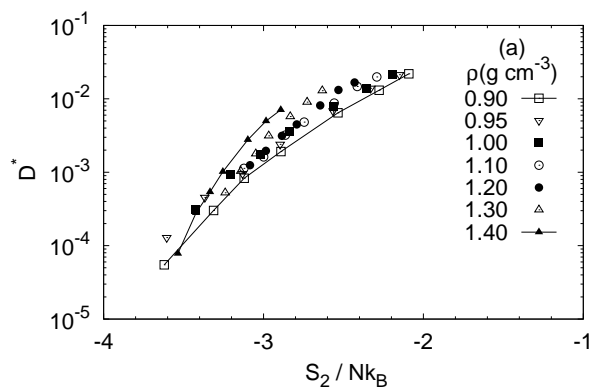


Figure 3.

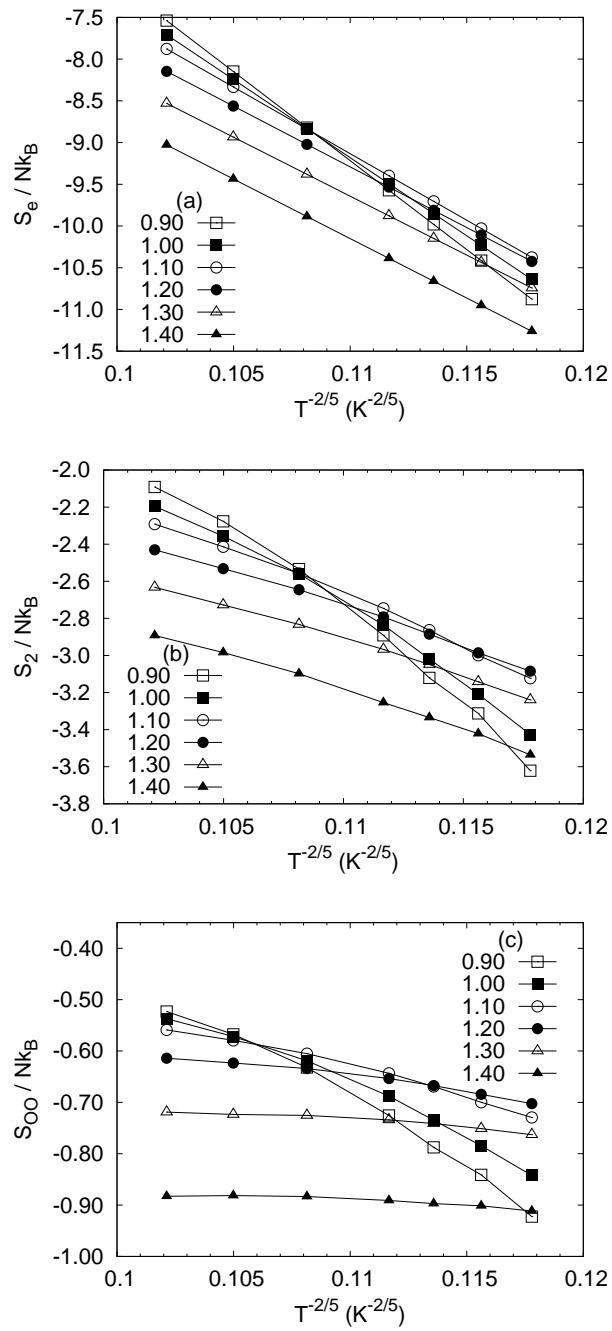


Figure 4.

	SPC/E [30]	TIP3P [31]	BeF ₂ [33]	SiO ₂ [34]	2SRP [16]
$\rho^m(\text{g cm}^{-3})$	1.01	0.98	1.8	2.3	1.5
$T^m(\text{K})$	251	195	2310	5000	0.0548

TABLE 1: State point corresponding to the maximum temperature along the TMD locus (ρ^m, T^m) for the systems studied. Potential parameters are given in the references. Values for the 2SRP are in the reduced units defined in the simulations details.